CONF-830562--2

DEVELOPMENTAL TECHNIQUES FOR ULTRASONIC FLAW DETECTION AND CHARACTERIZATION IN STAINLESS STEEL*

David S. Kupperman

Materials Science and Technology Division
Argonne National Laboratory
Argonne, Illinois 60439

CONF-830562--2

DE83 014282

April 1983

To be presented at the OECD/IAEA Specialist Meeting, Ispra, Italy, May 1983.

*Work supported by the U.S. Nuclear Regulatory Commission, Office of Nuclear Regulatory Research.

DEVELOPMENTAL TECHNIQUES FOR ULTRASONIC FLAW DETECTION AND CHARACTERIZATION IN STAINLESS STEEL*

David S. Kupperman

Materials Science and Technology Division
Argonne National Laboratory
Argonne, Illinois 60439

ABSTRACT

Flaw detection and characterization by ultrasonic methods is particularly difficult for stainless steel. This paper focuses on two specific problem areas: (a) The inspection of centrifugally cast stainless steel (CCSS) and (b) the differentiation of intergranular stress-corrosion cracking (IGSCC) from geometrical reflectors such as the weld root. To help identify optimal conditions for the ultrasonic inspection of CCSS, the effect of frequency on propagation of longitudinal and shear waves was examined in both isotropic and anisotropic samples. Good results were obtained with isotropic CCSS and 0.5-MHz angle beam shear waves. The use of beam-scattering patterns (i.e. signal amplitude vs skew angle) as a tool for discriminating IGSCC from geometrical reflectors is also discussed.

*Work supported by the U.S. Nuclear Regulatory Commission, Office of Nuclear Regulatory Research.

DEVELOPMENTAL TECHNIQUES FOR ULTRASONIC FLAW DETECTION AND CHARACTERIZATION IN STAINLESS STEEL*

David S. Kupperman

Materials Science and Technology Division
Argonne National Laboratory
Argonne, Illinois 60439

A. INTRODUCTION

Two major areas of difficulty in the ultrasonic inspection of stainless steel (SS) reactor components are (a) the inspection of centrifugally cast stainless steel (CCSS), which is used for piping in pressurized water reactors but is difficult to inspect reliably[1-5] because of its coarse grains; and (b) the detection of intergranular stress corrosion cracking (IGSCC),[6-11] especially in the vicinity of geometrical reflectors such as the weld root. In the first part of this study, CCSS samples were examined at frequencies as low as 0.5 MHz to identify optimal ultrasonic testing conditions for this material. Both isotropic and anisotropic samples were tested (the latter are transversely isotropic, owing to the presence of long columnar grains). In the second part, the scattering of ultrasonic waves was examined to determine whether the dependence of the reflected ultrasonic signal on skew angle could be used to distinguish IGSCC from geometrical reflectors in SS pipes.

B. CENTRIFUGALLY CAST STAINLESS STEEL

Two types of CCSS samples have been evaluated. These samples are both from cast Type 304 SS piping ∿27 in. (∿0.69 m) in diameter, but they have different microstructures. Sample A has large grains (1-2 mm in diameter) without columnar structure; sample B has large columnar grains (see Fig. 1). Experiments were performed to determine the degree of texturing in these samples. If the anisotropic CCSS looked ultrasonically like SS weld metal, then techniques developed for one material would also be applicable to the other. In addition, if the two specimens had different textures, they could be used to determine whether the inspectability of CCSS is related to the degree of anisotropy in the sample. Several specimens were cut from various places in samples A and B. These specimens were 10 x 10 x 50 mm, 15 x 15 x 65 mm, and 19 x 19 x 60 mm in size and provided acoustic path lengths of 20, 30, and 38 mm, respectively, for pulse-echo measurements of sound velocity and attenuation. Waves were propagated at 0, 45, and 90° to the z-axis (the direction perpendicular to the pipe axis); in sample B, as expected for anisotropic CCSS piping, the z-axis is also the columnar-grain axis. Data for each propagation direction were taken in three orthogonal planes using a Panametrics 2.25-MHz (1/2-in.) normal-incidence shear-wave transducer and shear-wave couplant, an Aerotech type gamma 2.25-MHz longitudinal-wave transducer, and a Panametrics 5052UAX ultrasonic analyzer. Transit times were measured on a Tektronix 7904 oscilloscope and 7B85 delaying time base. The oscilloscope was calibrated with a Type 184 Time Mark Generator. Transit times were measured by overlapping successive echoes, or main pulse and first echo if only one echo was detectable.

The results for sample A are shown in Fig. 2. Data are shown for propagation angles of 0, 45, and 90° and orthogonal planes xy, xz, and yz. Single-crystal elastic constants[1] were used to calculate the average longitudinal- and shear-wave velocities for this material. In an acoustically isotropic sample, these velocities will be observed regardless of propagation direction, as

indicated by the solid curves in Fig. 2. The sound velocity results for both longitudinal and shear waves are very consistent with the assumption of acoustic isotropy; no preferred texture is evident.

For sample B, on the other hand, velocities varied considerably with propagation direction. Sound velocity data for sample B are presented in Figs. 3, 4, and 5 for longitudinal, vertically polarized shear (SV), and horizontally polarized shear (SH) waves, respectively. The figures also show model predictions based on both transverse isotropic and single-crystal symmetry, calculated from single-crystal elastic constants given in Ref. 1. For all three wave modes, the data are consistent with the transverse isotropic model. In this respect, the columnar grain structure of sample B is acoustically similar to that of SS weld metal. The only difference of significance for ultrasonic NDE is in the size of the columnar grains (generally larger in CCSS). These results indicate that problems and solutions associated with SS weld metal are applicable to CCSS with columnar grains (and vice versa), although the large grains in the CCSS may result in higher grain-scattering attenuation than in SS weld metal.

The apparent attenuation in samples A and B was measured from the signal loss of two successive echoes. The results for longitudinal waves are presented in Table I. The lowest attenuation occurred in the anisotropic sample, for propagation at 45° to the grain axis. (Similarly, in SS weld metal, longitudinal waves undergo the least attenuation when propagated at 45° to the grain axes.[2]) The apparent attenuation was greater in the isotropic sample: In effect, this sample lacks the one available "window" for inspecting CCSS with longitudinal waves.

TABLE I. Apparent Attenuation (dB/cm) of Longitudinal Waves in CCSS

Sample	Propagation Direction Relative to Columnar Grains 0°	45°	90°
B (anisotropic)	5.5	3	7
A (isotropic)	Average for all directions: 5.7 ± 0.7		

In general, shear waves showed higher attenuation than longitudinal waves for the same frequency (smaller wavelength), and similar attenuation in isotropic and anisotropic material. Consequently, both materials were more difficult to inspect with shear waves than with longitudinal waves at the same frequency (2.25 MHz). Results for lower frequency shear waves are discussed in a later section.

Because the level of anisotropy in CCSS significantly affects the reliability and sensitivity of ultrasonic inspection, a method of rapidly determining this level would be very useful. In particular, one would like to be able to distinguish between isotropic structures and anisotropic ones in which the long axis of the columnar grains is in the pipe radial direction, as would be expected for anisotropic CCSS piping. Work has been initiated to establish whether sound velocity measurements can effectively provide this information for cast pipes. In principle, isotropic and anisotropic (columnar-grain) microstructures

can be differentiated by measuring the velocities of longitudinal and shear waves in various directions. In practice, for pipes, velocities of longitudinal waves propagating normal to the pipe surface (in the z-direction) are most readily measured. The velocity of longitudinal waves measured in the z-direction in the isotropic CCSS varied between 5850 and 6050 m/s. In the anisotropic material, the velocity in the z-direction (along the long axis of the grains) varied between 5400 and 5650 m/s. The theoretical value of the latter velocity is about 5100 m/s.[1]

This information suggests that for a propagation direction normal to the pipe surface, a low longitudinal-wave velocity (<5650 m/s) indicates that the sample is transverse isotropic or nearly so and a higher velocity (>5800 m/s), indicates isotropy. This concept was tested on a piece of welded CCSS pipe sent to us by Battelle Pacific Northwest Laboratories (PNL). The longitudinal sound velocity was measured on both sides of the weld with a 1-MHz, 1/2-in. Panametrics transducer. Generally, two echoes could be seen, and velocity was measured by overlapping the echoes and measuring the time between them. The velocities for the left and right sides were 5890 $\pm$ 40 and 5490 $\pm$ 30 m/s, respectively. These values fall within the previously determined ranges for isotropic material (5850-6050 m/s) and anisotropic (transverse isotropic) material (5400-5650 m/s), respectively. PNL notations on the pipe (initially covered with tape) confirmed the isotropic nature of the left side and the anisotropic (transverse isotropic) nature of the right side. In this initial test the thickness of the pipe (58.5 mm on the left side, 60.5 mm on the right) was measured to obtain the velocity, but it is possible to obtain the same results without a thickness measurement by using other ultrasonic modes and/or propagation directions. For example, if in addition to measuring transit times in the direction normal to the pipe surface, one also measured transit times for 45° longitudinal waves (see Fig. 6), knowledge of the pipe thickness would not be needed. From Fig. 6, the transit time for normal-incidence longitudinal waves is

$$t_N = \frac{2h}{V_{90°}} , \tag{1}$$

where t_N is the round trip time, h the pipe wall thickness, and $V_{90°}$ the longitudinal velocity for propagation normal to the pipe outer surface. For 45° longitudinal waves,

$$t_{RT} = \frac{2\sqrt{2}h}{V_{45°}} , \tag{2}$$

where t_{TR} is the time between transmitted and received pulses minus the transit time in the wedges, and $V_{45°}$ is the longitudinal velocity for a 45°-angle beam. Dividing Eq. (2) by Eq. (1), one obtains

$$R = \frac{t_{TR}}{t_N} = \frac{\sqrt{2}\, V_{90°}}{V_{45°}} . \tag{3}$$

For isotropic material it has been shown empirically that

$$V_{90°} = V_{45°} \pm 1.7\% ,$$

and thus

$$R_{isotropic} = 1.41 \pm 0.02 \quad .$$

For anisotropic material with the long axis of the columnar grains in the z-direction,

$$\frac{V_{45}}{V_{40}} = \frac{6.15 \pm 0.02}{5.5 \pm 0.1} = 1.12 \pm 0.08 \ ;$$

$$R_{anisotropic} = 1.59 \pm 0.08$$

This analysis suggests that in CCSS, isotropic and anisotropic microstructures may be distinguished by transit time measurements, independent of knowledge of wall thickness. Efforts are continuing to establish the reliability of this concept.

Angle beam testing in CCSS with columnar grains is often carried out with 1-MHz longitudinal waves propagating at approximately 45° to the long axis of the columnar grains, because a focusing effect occurs at this propagation angle for longitudinal (but not shear) waves. For isotropic CCSS, the problem reduces to one of increasing the ratio of wavelength to grain size. A 65-mm-thick block of isotropic CCSS (grain size of 1-2 mm) containing a 10-mm-deep EDM notch and a 6-mm-diam side-drilled hole was used to compare the effectiveness of shear and longitudinal waves. The sample is shown in Fig. 7. To match the 6-mm wavelength of 1-MHz longitudinal waves, a shear-wave frequency of 0.5 MHz was used. Figure 8 shows typical radio frequency signals obtained from the side-drilled hole (upper traces) and notch (lower traces) with normal-incidence shear waves (left) from a Panametrics 1/2-MHz, 1-in.-diam transducer and normal-incidence longitudinal waves (right) from a Panametrics 1-MHz, 1/2-in.-diam transducer; the transducers were placed on the "slope" of the sample to generate the equivalent of 45°-angle beams.

The results indicate that for comparable wavelengths, shear and longitudinal waves generate comparable signals for a side-drilled hole. However, for the notch, the reflection generated by the 0.5-MHz shear wave is much stronger than that for the 1-MHz longitudinal waves. The loss of signal for the longitudinal waves is the result of mode conversion at the notch. These results, although limited, suggest that angle beam testing at 0.5 MHz may be the choice for inspecting isotropic CCSS with grain sizes in the range of 1-2 mm. The sensitivity for these lower frequency shear waves is, of course, lower because of the long wavelengths; therefore, only relatively large flaws will be detectable. Note that the polarization of the shear wave can be varied by rotating the transducer. As one might expect for isotropic CCSS, varying the polarization had relatively little effect on reflected echoes.

The effect of lowering the frequency of the shear waves from 1 to 0.5 MHz can be seen in Fig. 9. Here, 45° shear waves were generated with Panametrics 1-in.-diam transducers on plastic wedges. For a 25-mm-thick wrought plate, comparable signals were obtained from the corner at both frequencies with a 1V acoustic path (top). For the isotropic half of a piece of 27-in.(0.7-m)-diam welded pipe (60 mm thick), insonified along a 1/2V path, a signal was observed at 0.5 MHz (bottom left), whereas none was seen at 1 MHz (bottom right). No signals were seen when the anisotropic half of the specimen was interrogated.

C. ULTRASONIC DETECTION OF IGSCC

As is well known, one of the main obstacles to reliable ultrasonic detection of IGSCC is the difficulty in distinguishing these cracks from geometrical reflectors. One possible approach to this problem is to look for differences in the dependence of echo amplitude on the angle of incidence of the ultrasonic beam on the reflector surface. Because IGSCC has an irregular and generally branched character, it might be expected to produce a broader scattering pattern than that of a geometrical reflector.

Seven cracks and four geometrical reflectors in Type 304 SS specimens were examined with 2.25-MHz, 45° shear waves (by use of a 1/4-in. miniature shear-wave transducer from Aerotech) in a pulse-echo mode. A Sonic Mark I pulser-receiver was employed for data acquisition. Figure 10 illustrates the experimental arrangement and shows how the skew angle θ was measured. The echo amplitude (expressed as the gain setting required to bring the echo height to 80% of the full screen height) was plotted against θ by peaking the signal for each θ; Fig. 11 schematically illustrates the resultant plot. The variation in signal with θ was quantified by measuring the "full width at 3/4 maximum signal" (FW3/4M) for the curves, as shown in Fig. 11. Figure 12 describes the specimens and gives the results. The maximum echo amplitudes for all the reflectors were of the same order of magnitude; however, the FW3/4M values for the cracks, as a group, differed from those of the geometrical reflectors. For the cracks, the FW3/4M values ranged from 50° to 70°; for the geometrical reflectors, they ranged from 26° to 38°. The lower values of FW3/4M for the geometrical reflectors correspond to a sharper change in echo amplitude with θ. These results represent only a limited number of samples, but if the type of information discussed here can be acquired in the field (perhaps by a multi-element probe), the chance of distinguishing cracks from geometrical reflectors may be improved. This phenomenon will be further quantified by use of the pitch-catch mode and additional samples.

A probe has been designed that can be used with a multiscanner to provide data needed for IGSCC discrimination. The requirements for such a "multiple-element skew angle" probe include (1) uniform coupling of many wedges and (2) a small enough size to avoid interference with the weld crown. The initial design (Fig. 13), aimed toward inspection of 27-in.(0.7-m)-diam pipes, uses seven crystals with a multiscanner and individual gain control for each channel. The gain for each element can be adjusted to compensate for the drop in echo amplitude with skew angle that characterizes geometrical reflectors. After the gain of the pulser-receiver is adjusted to the calibrated level, IGSCC could in principle be identified by the presence of above-threshold echo signals for the transducers positioned at large skew angles; the signals generated at large skew angles by a geometrical reflector will fall below the threshold. When the probe is completed, it will be tested on pipes containing geometrical reflectors as well as IGSCC to establish the reliability of the concept.

D. SUMMARY

The present results show that the attenuation of ultrasonic waves is not necessarily lower in isotropic CCSS than in anistropic CCSS; this is because anisotropic material provides a "window" of low attenuation for longitudinal waves propagating at about 45° to the columnar grains, whereas isotropic material does not. If isotropic CCSS (with grains of the order of 1-2 mm) is to be inspected, the results of this study suggest that 0.5-MHz shear waves would

provide the best combination of penetration and sensitivity; they would give a high ratio (3-6) of wavelength to grain size, and would produce minimal mode conversion problems compared with longitudinal waves. For anisotropic material, 1-MHz longitudinal waves appear to be optimum.

Other data presented here suggest that it may be possible to distinguish IGSCC from geometrical reflectors by analysis of the dependence of echo amplitude on skew angle. A conceptual design was presented for a probe to carry out this analysis in the field.

ACKNOWLEDGMENTS

The author wishes to thank S. Doctor of Battelle Pacific Northwest Laboratories for providing the cast stainless steel, M. Behravesh of the Electric Power Research Institute for graphite-wool-grown IGSCC specimens, and R. Lanham of Argonne National Laboratory for assistance in acquiring the data presented here.

REFERENCES

1. D. S. Kupperman and K. J. Reimann, Ultrasonic Wave Propagation and Anisotropy in Austenitic Stainless Steel Weld Metal, IEEE Trans. Sonics Ultrason. SU-27(1), 7-15 (January 1980).

2. S. Matsumoto and K. Kumura, The Relationship Between Grain Size and Ultrasonic Attenuation Coefficient in Austenitic Stainless Steel and Iron, Trans. Natl. Res. Inst. for Metals 14(4), 155-164 (1972).

3. I. N. Ermolov and B. P. Pilin, Ultrasonic Inspection with Coarse Grain Anisotropic Structures, NDT Intl. 9(6), 275 (1976).

4. D. S. Kupperman, K. J. Reimann, and N. F. Fiore, Role of Microstructure in Ultrasonic Inspectability of Austenitic Stainless Steel Welds, IEEE Trans. Sonics Ultrason. SU-27(1), 7 (1980).

5. B. R. Dewey, L. Adler, R. T. King, and K. V. Cook, Application of Anisotropic Elasticity to Centrifugally Cast Piping, Oak Ridge National Laboratory Report ORNL/TM-5994 (October 1977).

6. A. R. Whiting, A. Greer, and J. McElroy, The Difficulties of Applying Nondestructive Evaluation to Stainless Steel Components in the Nuclear Industry, presented at Int. Conf. on NDE in the Nuclear Industry, Salt Lake City, UT (February 13-15, 1978).

7. H. Wustenberg and E. Mundry, Limiting Influences on the Reliability of Ultrasonic In-Service Inspection Methods, in Inst. Mech. Engrs. Conference Publication 8 (1974).

8. P. Singh and J. Rose, The Dual Element Angle Beam Transducer, Paper Summaries, ASNT Fall Conference, October 15-18, 1979, St. Louis, MO, p. 197.

9. F. L. Becker, Ultrasonic Inspection Reliability for Primary Piping Systems, presented at CSNI Specialists Meeting on Reliability of Ultrasonic Inspection of Austenitic Stainless Steel Components, Brussels, Belgium (May 29-30, 1980).

10. J. L. Jackson, Program for Field Validation of the Synthetic Aperture Focusing Technique for Ultrasonic Testing (SAFT UT), Midyear Progress Report, Southwest Research Institute Report NUREG/CR-0290 (July 1978).

11. A. N. Mucciardi, Automatic Detection and Sizing of IGSCC from Ultrasonic RF Signal Analysis, presented at 3rd Int. Conf. on NDE in the Nuclear Industry, Salt Lake City, UT (February 11-13, 1980).

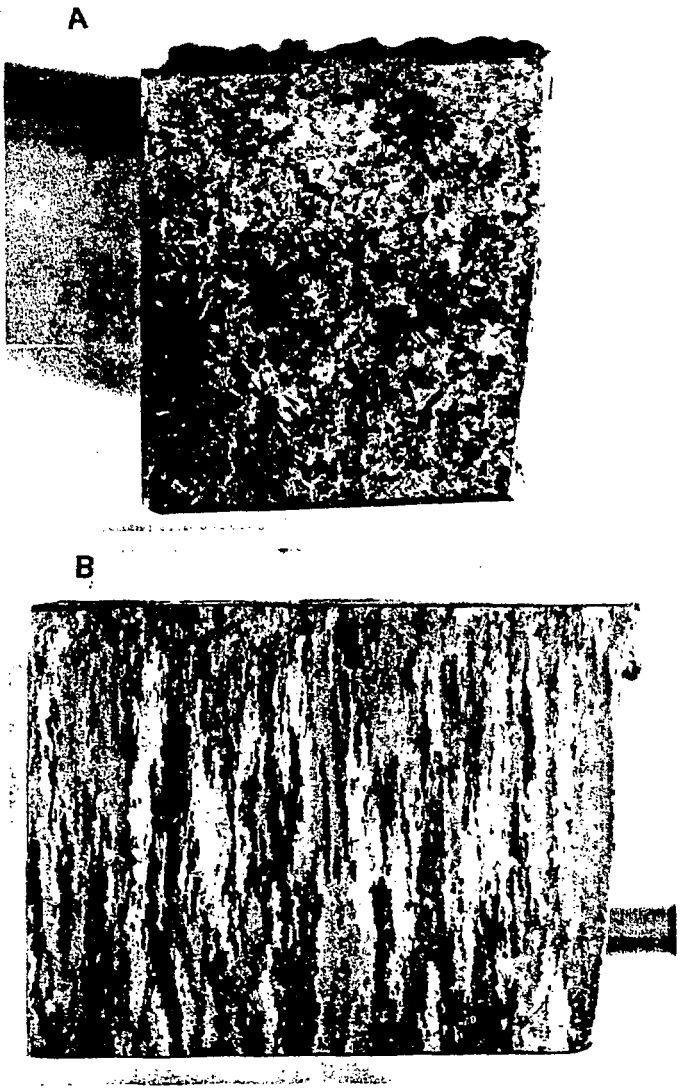

Fig. 1. Photographs of Etched Centrifugally Cast Stainless Steel Samples A and B. Sample B is ∿85 mm across. Columnar grains are present in sample B only.

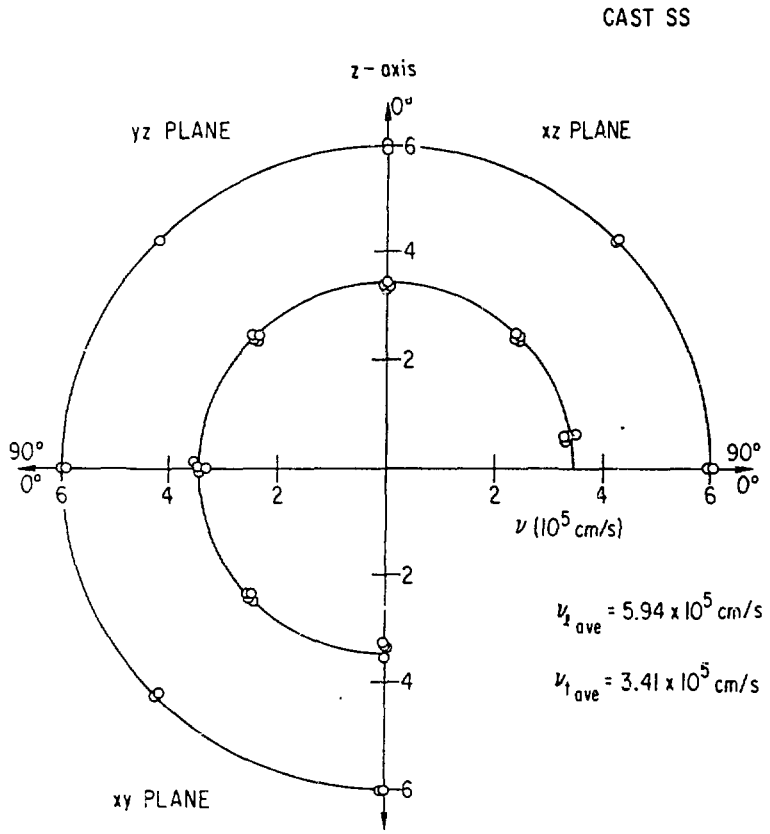

Fig. 2. Sound Velocity of Longitudinal (v_ℓ) and Shear (v_t) Waves vs Propagation Direction in CCSS Sample A. Solid curves are average values based on the assumption that the specimen is isotropic.

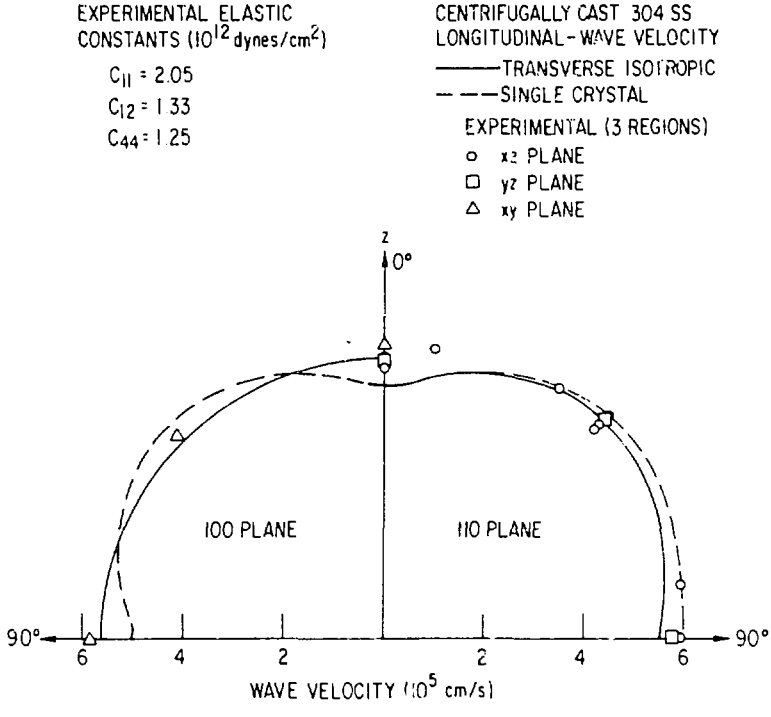

Fig. 3. Sound Velocity of Longitudinal Waves vs Propagation Direction in CCSS Sample B, for {100} and {110} Planes. The z axis is the preferred <100> crystallographic direction in sample B. Also shown are theoretical curves for single-crystal (cubic) and transverse isotropic symmetry.

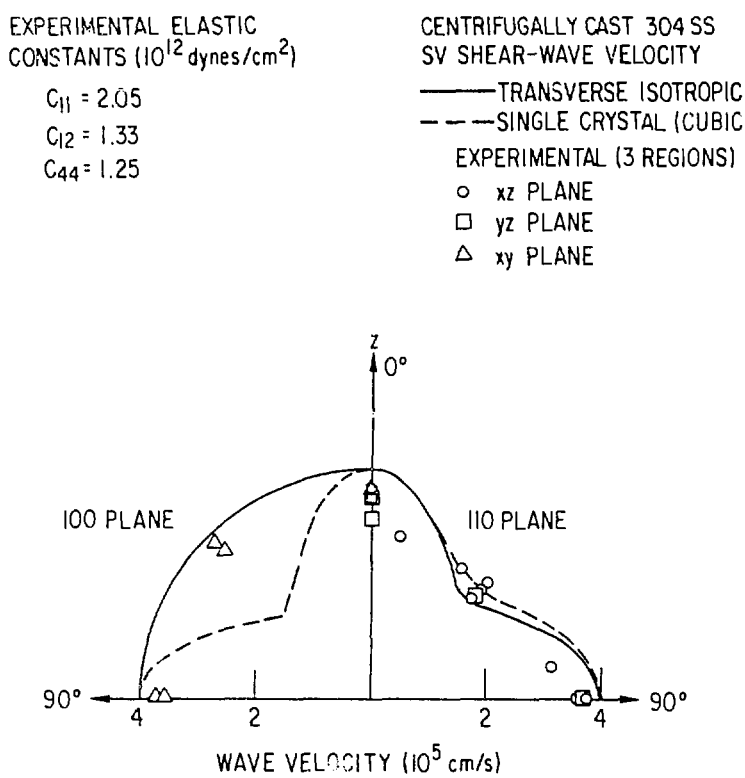

Fig. 4. Sound Velocity of SV Waves vs Propagation Direction in CCSS Sample B, for {100} and {110} Planes. The z axis is the preferred <100> crystallographic direction. Also shown are theoretical curves for single-crystal (cubic) and transverse isotropic symmetry.

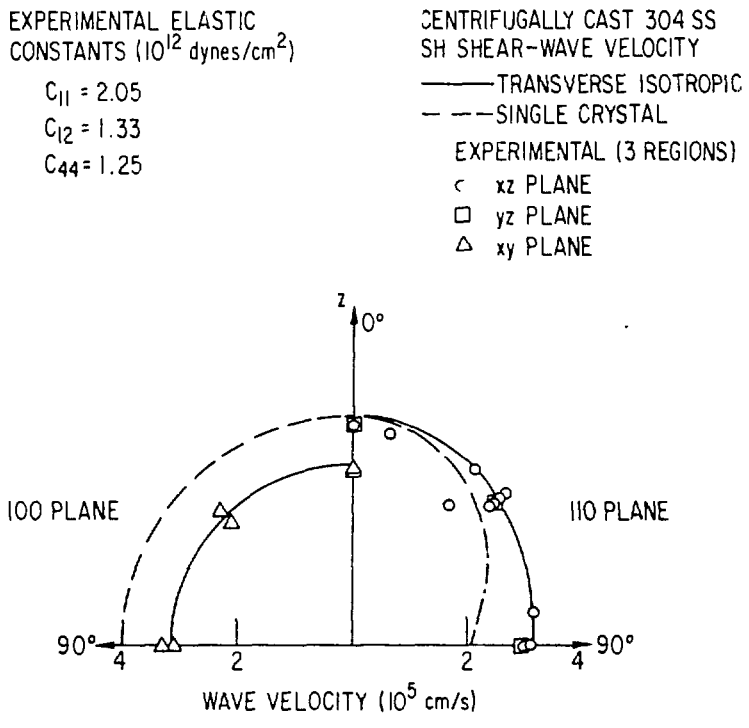

Fig. 5. Sound Velocity of SH Waves vs Propagation Direction in CCSS Sample B, for {100} and {110} Planes. The z axis is the preferred <100> crystallographic direction. Also shown are theoretical curves for single-crystal (cubic) and transverse isotropic symmetry.

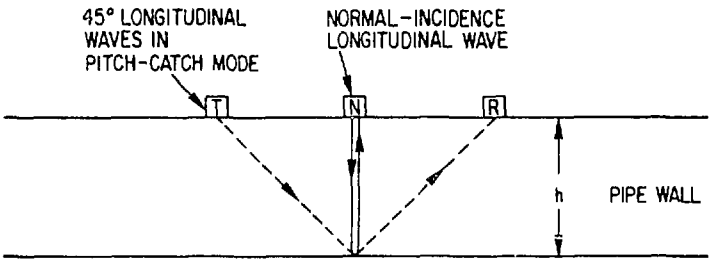

$$t_N = \frac{2h}{V_{90°(\ell)}} \qquad t_{TR} = \frac{2\sqrt{2}\,h}{V_{45°(\ell)}}$$

$$R = \frac{t_{TR}}{t_N} = \frac{\sqrt{2}\,V_{90°(\ell)}}{V_{45°(\ell)}}$$

Fig. 6. Schematic Design Showing Wall of CCSS Pipe and Location of Transducers for Generating Normal-Incidence and 45° Angle Beam Longitudinal Waves. Transmit-receive (minus transit time in wedge) and pulse-echo times are indicated as a function of wall thickness and velocity.

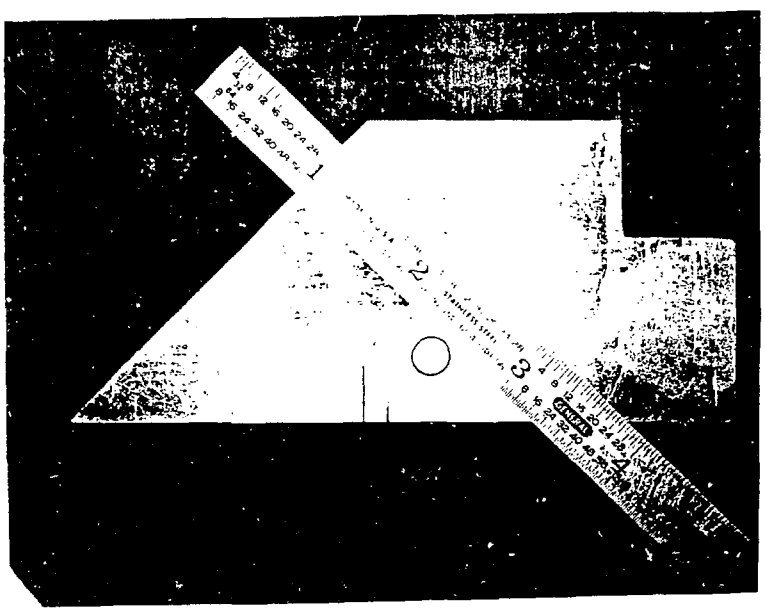

Fig. 7. Photograph of Isotropic CCSS (Grain Diameter of 1-2 mm) Containing EDM Notch and 6-mm-diam Side-drilled Hole. The sample is 65 mm thick.

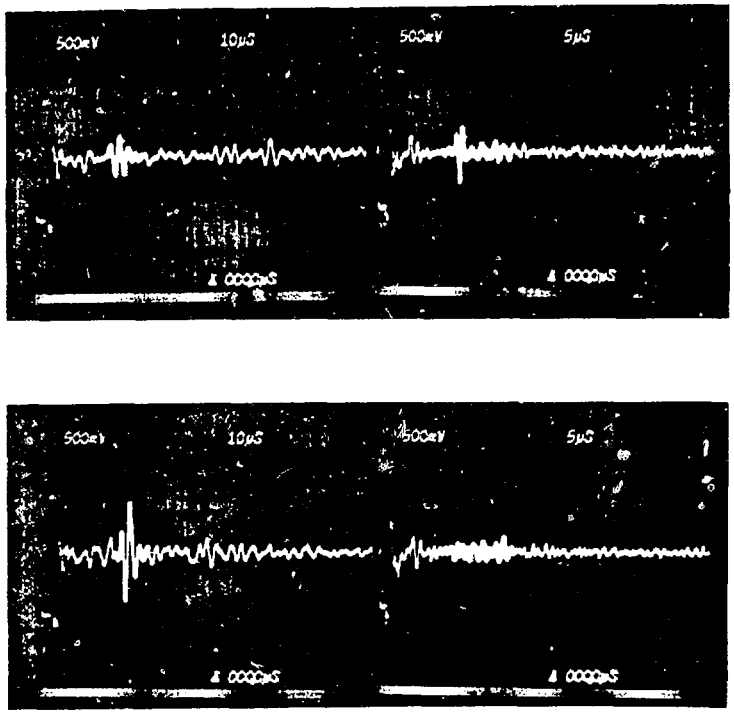

Fig. 8. Radio Frequency Echo Signals from Isotropic CCSS Sample of Fig. 7. Signals from (top) side-drilled hole and (bottom) EDM notch were obtained with (left) 0.5-MHz shear waves and (right) 1.0-MHz longitudinal waves. Transducers were placed on the sloping side of the sample to simulate 45°-angle beams.

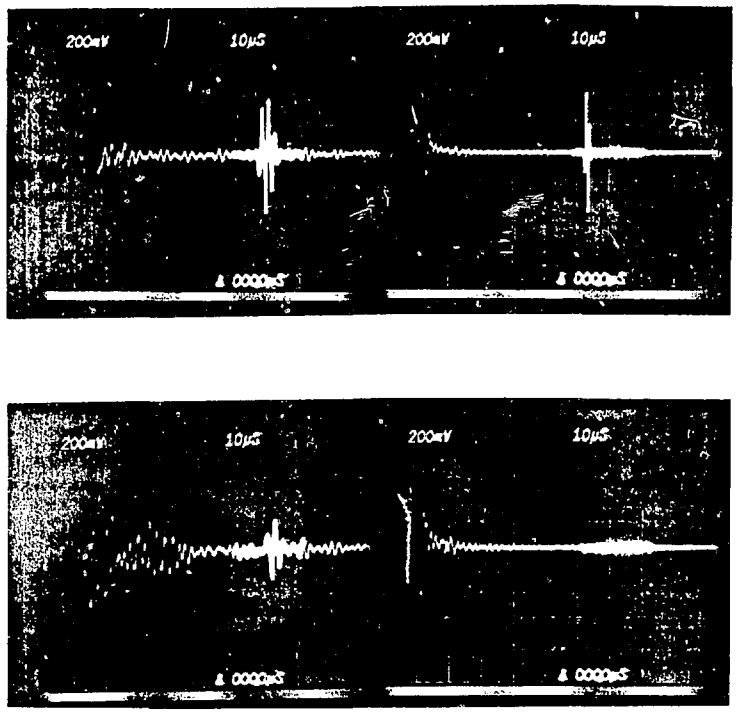

Fig. 9. Radio Frequency Echo Signals from Corner Reflectors in (Top) a 25-mm-thick Plate of Small-grained Wrought SS, Insonified along 1V Path, and (Bottom) a 27-in.-diam. Pipe Section of Isotropic CCSS, Insonified along 1/2V Path. Signals were obtained with (left) 0.5-MHz and (right) 1.0-MHz shear waves.

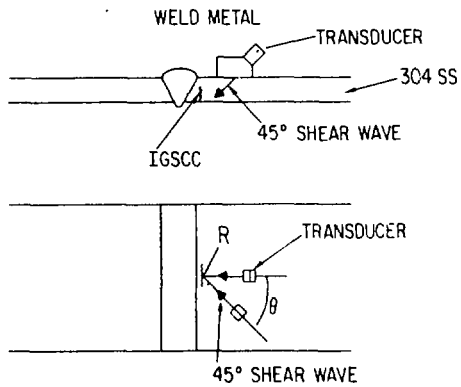

Fig. 10. Diagram of Experimental Arrangement for Ultrasonic Interrogation of IGSCC and Geometrical Reflectors in Type 304 SS Specimens. From its initial position on beam path 1, the transducer is moved in an arc on the pipe surface to a position on beam path 2 such that the acoustic path length from the transducer to the reflector plane (point R) remains constant. The skew angle θ is the angle between the projections of beam paths 1 and 2 onto a plane tangent to the pipe surface at the initial transducer position.

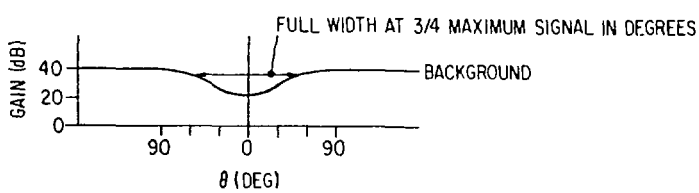

Fig. 11. Schematic of Data Representation Obtained by Plotting Echo Amplitude (Expressed as System Gain Needed to Bring Echo Height to 80% of Full Screen Height) vs Skew Angle θ. The arrow shows how the FW3/4M value is obtained from such a plot.

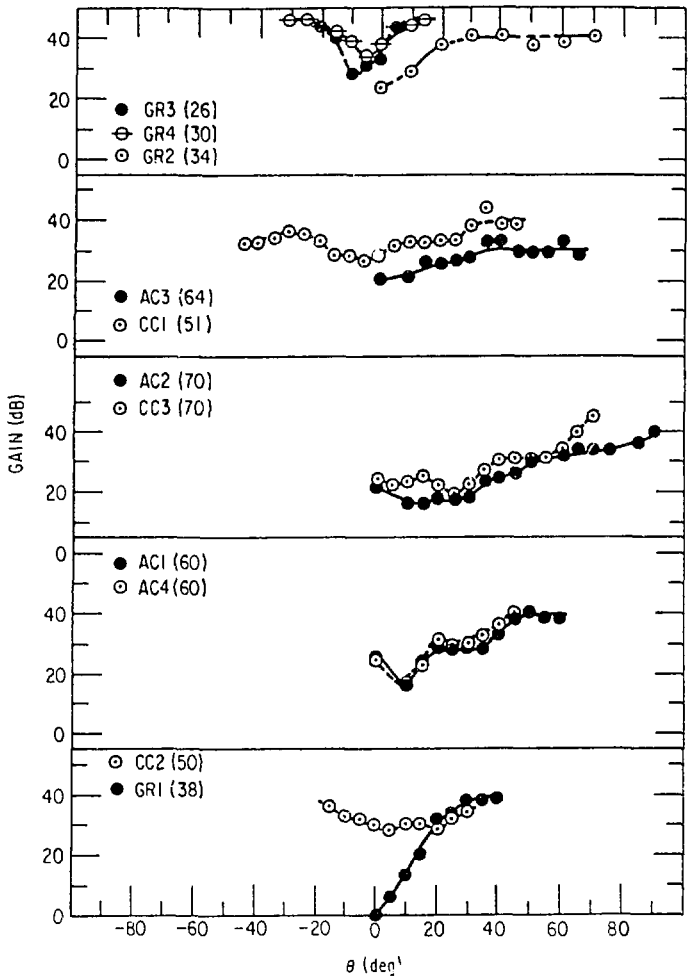

Geometrical Reflectors	
GR1:	End of 12-in. pipe
GR2:	EDM notch (6 mm long, 2 mm deep) in 25-mm-thick plate
GR3:	Weld root in 12-in. pipe
GR4:	Weld root in 20-in. pipe

IGSCC	
AC1-AC4:	Graphite-wool-grown axial cracks in 12-in. pipe
CC1,CC2:	Graphite-wool-grown circumferential cracks in 12-in. pipe
CC3:	Field-induced circumferential crack in 10-in. pipe

Fig. 12. Echo Amplitude vs θ for Seven IGSCC and Four Geometrical Reflectors in Type 304 SS Specimens. Numbers in parentheses are FW3/4M values determined from these curves (see Fig. 11). Specimens CC1, CC2, and AC1-AC4 were provided by EPRI's Nondestructive Evaluation Center.

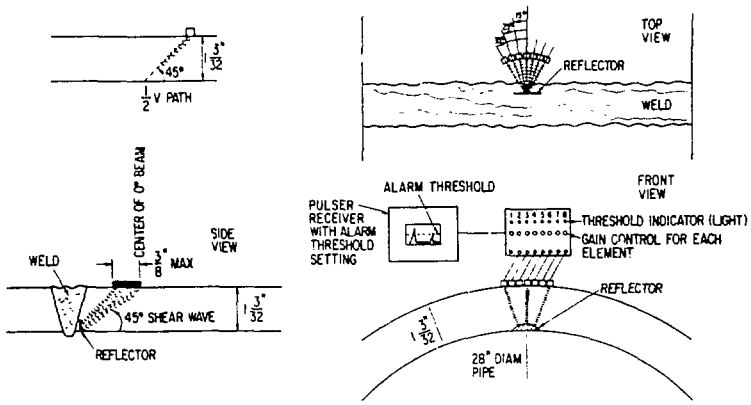

Fig. 13. Schematic Diagram Showing Inspection of a Pipe Heat-affected Zone with a Multielement Probe Designed to Detect Variations in Echo Signal Amplitude with Skew Angle.